In-situ coating of leather with conducting polyaniline in colloidal dispersion mode

In-situ coating of leather with conducting polyaniline in colloidal dispersion mode

Fahanwi Asabuwa Ngwabebhoh,[1] Oyunchimeg Zandraa,[1] Tomáš Sáha[1], Jaroslav Stejskal,[1,2,*] Miroslava Trchová,[2] Dušan Kopecký,[2] Jiří Pfleger,[3] Jan Prokeš[4]

[1] University Institute, Tomas Bata University in Zlin, 760 01 Zlin, Czech Republic

[2] University of Chemistry and Technology, Prague, 166 28 Prague 6, Czech Republic

[3] Institute of Macromolecular Chemistry, Academy of Sciences of the Czech Republic, 162 06 Prague 6, Czech Republic

[4] Charles University, Faculty of Mathematics and Physics, 180 00 Prague 8, Czech Republic

[*]**Corresponding author:** E-mail: stejskal@utb.cz (J. Stejskal)

Abstract

Four different leathers and a nonwoven fibrous mat have been coated with a conducting polymer, polyaniline, in-situ during the oxidation of aniline hydrochloride in the presence of poly(*N*-vinylpyrrolidone) stabilizer. This colloidal dispersion approach prevented the undesirable formation of free polyaniline precipitate outside the leather fibres. The molecular structure of polypeptide fibres with deposited polyaniline is discussed on the basis of FTIR spectra. Raman spectroscopy confirmed that individual fibres were coated with a conducting polymer. The cross-sectional optical microscopy revealed that the leather was coated on both sides. The layer thickness, tens to hundreds micrometres, was determined by the penetration depth of reaction mixture. In the case of diabetic insole mat gambrela, polyaniline penetrated throughout the sample body. This was also confirmed by the measurement of transversal resistance. The typical sheet resistance was in units to hundreds kΩ sq^{-1} and differed but was of the same order of magnitude on top and bottom sides. The samples were subject to cyclic bending and of the resistivity changes have been monitored. Antibacterial activity of some leathers improved after the coating with polyaniline.

Keywords: Polyaniline; Conducting composites; Conducting leather; Bending tests; Sheet resistance

1. Introduction

Natural polymers have often been a component of composite materials due to their environmental friendliness, ecological sustainability, biodegradability and biocompatibility. They have been combined with synthetic polymers that provided mechanical properties and value-added features, when electrical conductivity may serve as an example [1]. Polyaniline and polypyrrole have been the most frequent conducting composite components because of the ease of preparation at economic cost [2]. Such composites found uses especially in supercapacitors and as electrode materials [3] but their application range is much broader [4].

Polypeptides are important class of biopolymers that constitute a fundamental part of leather, a material widely used in clothing and shoes industry, which has been combined with polyaniline. For example, the macroporous aerogel based on sheep-skin-derived leather waste and poly(vinyl alcohol) was used as a substrate for the in-situ deposition of this conducting polymer [5]. The resulting material was tested for flame retardation and electromagnetic radiation shielding. There is, however, more attractive future when modified leather is used as a substrate with excellent mechanical and utility properties, e.g., in shoe/footwear industry.

So far, for instance, polyaniline/carbon nanotubes composition was screen-printed on leather to obtain a resistive heating element for car seats [6]. In another study, in-situ polymerization of aniline in the presence of goat leather yielded a material applicable as dry electrodes with antibacterial properties for electroencephalography [7]. Similar deposition of polyaniline on sheep leather was proposed to be useful in operating touch-screen devices [8, 9]. In addition to electrical properties, conducting polymers have also been offered as replacement of dyes in leather finish, brown-to-black for polypyrrole [8] or blue-to-green for polyaniline [9].

The *in-situ* deposition of polyaniline on various substrates is probably the only viable way to introduce the conducting polymer to leather. As a rule, the substrate to be coated is simply immersed in the aqueous reaction mixture containing aniline monomer and a suitable oxidant, typically ammonium peroxydisulfate [2, 10]. Despite the simplicity of the process, the protocol has to be controlled to ensure the uniform coating and distribution of polyaniline within the substrate, here a porous leather, and to reduce the contamination by macroscopic polyaniline precipitate adhering to the surface. These issues are discussed in the present contribution.

2. Experimental

2.1. Leathers

Five samples were selected for this study, (1) purple goatskin, (2) yellow-green pigskin, (3) gambrela diabetic insole mat, (4) light beige pigskin, and (5) natural beige pigskin. With the exception of sample 3, these materials are chrome-plated dyed substrates modified by graining the pigskin back to increase the evenness of colouring and softness. Their average thickness ranges between 0.5 to 0.9 mm. The leathers are intended and sorted for use as lining parts of footwear. Sample 3, is a nonwoven fibrous mat used as a step-on part for diabetic insoles [11]. In conjunction with whipped latex insole part, this mat can be recommended even for diabetics because in contact with the foot may reduce difficulties in vascular, orthopedic complications and improves thermal insulation properties of the footwear. However, the modification of these different materials with substrates like conducting polymers can improve performance, such as preventing the formation of microorganisms and fungi, thereby preventing diseases of the feet and their odour [12, 13].

2.2. Polyaniline coating

The pieces of leather have been coated in-situ with conducting polymer in so-called standard dispersion mode [14–16]. Aniline hydrochloride (2.59 g, 20 mmol; Sigma-Aldrich) were dissolved in 4 wt% aqueous solution of poly(*N*-vinylpyrrolidone) (molecular weight 360,000; Fluka, Switzerland) to 50 mL volume. Ammonium peroxydisulfate (5.71 g, 25 mmol; Lachner, Czech Republic) was separately dissolved in water to 50 mL. Both solutions were mixed at room temperature and poured over the leather samples placed in Petri dish. The concentrations of the chemicals in the reaction mixture thus was: 0.2 M aniline hydrochloride, 0.25 M ammonium peroxydisulfate and 2 wt% poly(*N*-vinylpyrrolidone). The care was taken so that the reaction mixture was in good contact both with top and bottom sides of immersed samples. After 1 h polyaniline-coated samples were removed, briefly immersed in 0.2 M hydrochloric acid, then in ethanol, until no coloration of the medium was seen, and finally left to dry in open air.

2.3. Surface morphology

Scanning electron microscopy (SEM) was performed with a scanning ultrahigh-resolution microscope MAIA3 Tescan (Brno, Czech Republic) to observe the morphology of leathers. Optical images were collected with a digital microscope of high degree magnification

Leica DVM2500 (Leica Microsystems, Germany) in order measure the thickness of the conducting layer of leathers. Typical polyaniline is dark green. Visualization was performed under diffuse light mode, which allows good visibility of the layers. Images ware taken at 100× magnification. The thickness on both sides was determined at five different points and the average value is reported in mean ± standard deviation format, analyzed using Analysis of Variance (ANOVA). Statistical significance was evaluated at p-value ≤ 0.05.

2.4. FTIR and Raman spectroscopies

Attenuated total reflection infrared (ATR FTIR) spectra of the leather samples were recorded using Nicolet 6700 spectrometer (Thermo-Nicolet, USA) equipped with reflective ATR extension GladiATR (PIKE Technologies, USA) with diamond crystal. Spectra were recorded in the 4000–400 cm^{-1} region with a deuterated L-alanine-doped triglycine sulfate detector at resolution 4 cm^{-1}, 64 scans and Happ-Genzel appodization. The spectra were corrected for carbon dioxide and humidity in the optical path.

Raman spectra were collected using a Thermo Scientific DXR Raman microscope equipped with 780 nm laser (power 4 mW). The spot size of the lasers was focused by 50× objective. The scattered light was analyzed by a spectrograph with holographic grating 1200 lines mm^{-1}, and a pinhole width of 50 μm. The acquisition time was 10 s with 10 repetitions.

2.5. Electrical properties

The resistivity was determined on top side by four-point van der Pauw method on circles 10 mm in diameter cut from polyaniline-coated leather. A Keithley 2010 multimeter, a current source Keithley 220, and a Keithley 705 scanner equipped with a matrix card Keithley 7052 were included in the setup.

Alternatively, the sheet resistance was measured by a linear four probe method using Jandel cylindrical four point probe, with current probes connected to a serial connection of K230 power supply and K196 multimeter as a current source, and potential probes connected to K181 for the voltage drop measurement (all devices from Keithley Instruments, USA). The tungsten carbide needle probes, 0.4 mm in diameter and the mutual distance 1.59 mm probe to probe, were applied on the surface of the tested material with the load adjusted within the range 60–150 g. The current was low to keep the dissipated energy below 50 μW. The Jandel probe was located at three different places within the inner area of the 13 mm wide rectangular samples of various length 17–35 mm. At each location the I–V characteristics were recorded for increasing and decreasing voltage and the surface resistance was calculated as the average

value of surface resistances from the linear part of the I–V characteristics according to the formula $R_{SR} = 4.53 \times U/I$, assuming that the thickness of the conducting layer is much smaller than the distance between the probes.

Transverse resistance was determined on samples with 0.5×1 cm^2 size. All four edges of samples were carefully cut-out prior to measurement to avoid any shortcuts on sides. Two-point measurement of resistance was carried with a 34401A multimeter (Hewlett Packard Inc., USA).

2.6. Bending tests

A novel tester allowing cyclic testing of electrical properties of leather samples during repeated bending has been constructed for the purpose of this work (Figure 1). This can mimic the movement of samples during walking if used in shoes. Here, a sample of size 1×2 cm^2 was attached to the flexible cantilever equipped with two measuring electrodes. The cantilever was fixed to a laboratory stand through specially designed stiff holder and the loose side of the cantilever was mechanically linked to a precise and strong servo-motor. The movement of the servo-motor, i.e., the bending angle of the cantilever were set through a control system designed in LabVIEW (National Instruments) and actuated by myRIO device (National Instruments). DC electrical resistance was followed by voltage divider connected to NI myRIO. The tester allows the cyclic bending of the sample with the user-selected frequency and total testing time. The user is also allowed to set the bending angle. In this work, 500 cycles with a cycle duration 20 s and the angle of bending 10° were set as an initial step allowing slow observation of processes and material relaxation taking place in the sample during the mechanical stress. The measured data were processed by a software made in Matlab (MathWorks, Inc.).

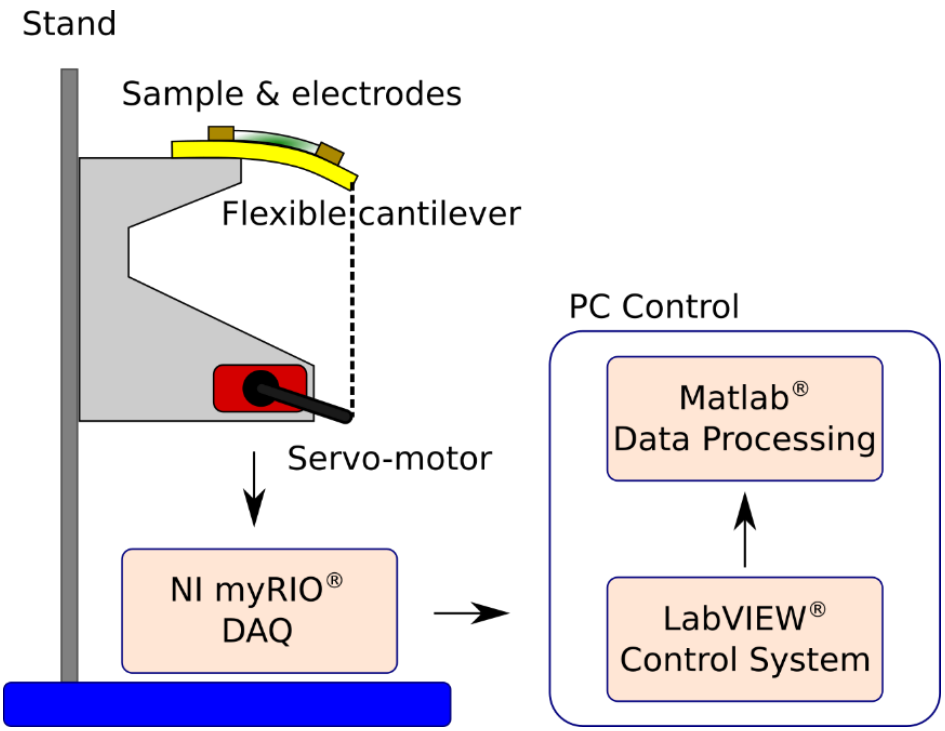

Figure 1. The bending tester for cyclic testing of electrical properties of leather samples under the stress.

2.7. Antibacterial properties

Two bacterial species of *Staphylococcus aureus* CCM 4516 and *Klebsiella pneumonia* CCM 4415 strains (obtained from the Czech Republic Centre for Collection of Microorganisms) were used to evaluate the antibacterial activity of original and coated leathers. The test was performed according to the standard ČSN 79 3880 for testing of antimicrobial properties of materials and products in leather industry. The test samples were cut in spherical shapes of diameter 10 mm and sterilized. The antibacterial activity was subsequently detected by the agar disc diffusion test. Bacterial suspensions of each bacteria stock of approximate concentration 9×10^{8} CFU mL^{-1} were inoculated onto the surface of prepared agar plates. The sterilized leather samples were placed on the surface of inoculated plates and incubated for 12 h at 37 °C. After 12 h, the test samples were removed and the agar plates were kept for another 24 h. The antibacterial activity was then determined by visualization of the agar plates under an Interscience Scan 500 Inhibition zone reader to determine the bacteria growth density.

3. Results and discussion

3.1. Polyaniline coating

In the in-situ coating of leather with polyaniline reported in the literature [9], when leather was penetrated with aniline hydrochloride solution and subsequently immersed in the solution of ammonium peroxydisulfate oxidant. Such approach affords the efficient deposition of polyaniline on leather threads [17] but the distribution of polyaniline within the leather volume is likely to be uneven because the aniline polymerization takes place preferentially at leather surface where both reactants meet and may be reduced or absent in the interior [18]. Adhering polyaniline precipitate that is produced at the surface of leather is easily peeled off (Figure 2a), makes the surfaces in contact dirty [16] and manifests itself also in reduced colour fastness [9]. This is also confirmed with a peel-off test with adhesive tape when no polyaniline is transferred to the tape.

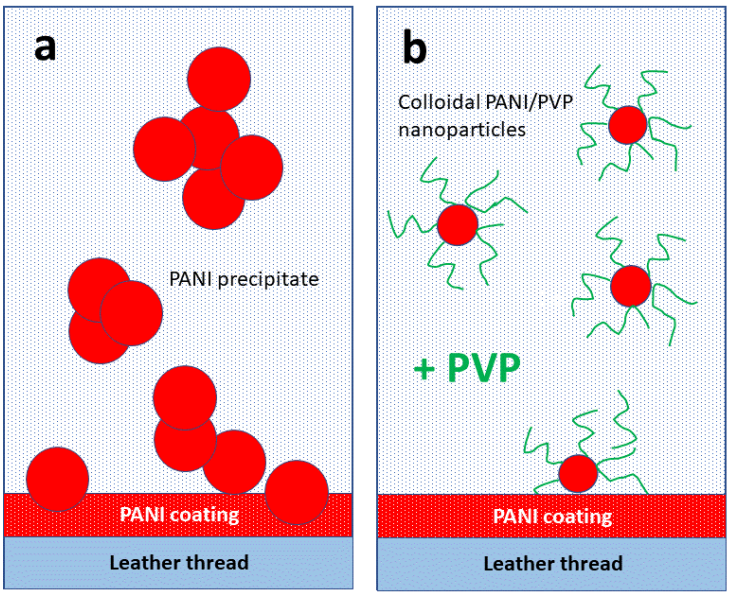

Figure 2. (a) Leather is accompanied by a macroscopic polyaniline precipitate during the standard deposition. (b) In the presence of poly(*N*-vinylpyrrolidone) (PVP), the colloidal nanoparticles are produced instead.

Leathers have the microstructure composed of collagen fibres (Figure 3), which varies for the individual types of leather. The first problem, the uneven distribution of the conducting polymer within the coated matrix, could be generally solved by the single-step immersion of the substrate in the reaction mixture containing both reactants. Although this approach was used in the present study, the complete homogeneity of the composite was not achieved, and the depth of polyaniline-coated leather phase was limited by the penetration of the aqueous reaction

mixture into leather within the time allocated for the polymerization of pyrrole, here of the order tens of minutes. It is also obvious that the penetration will depend on the hydrophilicity of the leather surface and size of the pores between the individual collagen fibres.

The drawback of adhering macroscopic precipitate was prevented in the present study by the coating deposition in the so-called dispersion mode, i.e. when the polymerization of aniline takes place in the solution of poly(*N*-vinylpyrrolidone) stabilizer [14, 15, 10], instead of water. The coating of leather is obvious to the naked eye as the change of any original leather colour to dark green. Under such conditions, colloidal polyaniline particles of submicrometre size are produced instead of macroscopic polyaniline precipitate [16]. The typical size of colloidal particles is 100–200 nm [10]. Colloidal polyaniline particles, which are generated in the surrounding solution (Figure 2b) in addition to the polyaniline coating of leather, are easily removed by washing and do not contaminate objects in later contact with dry leather. The absence of the precipitate is demonstrated on electron micrographs (Figure 4) and only some colloidal particles are still seen to adhere to polyaniline coating as very small dots at higher magnification (Figure 4; sample 3, left). Due to the presence of poly(*N*-vinylpyrrolidone), however, they are fastened to polyaniline coating and do not interfere in the applications. This is in the contrast to a macroscopic polyaniline precipitate, which is easily separated from leather surface [16].

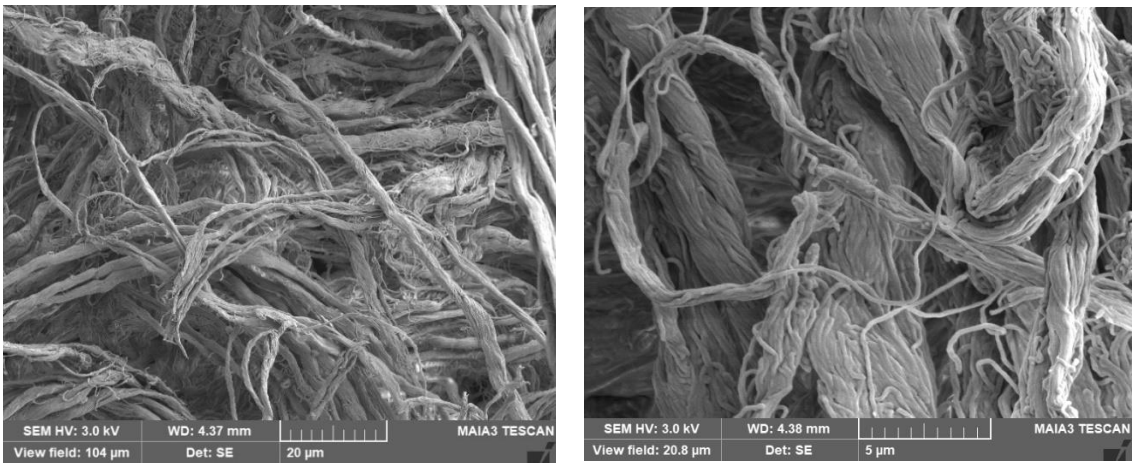

Sample 1

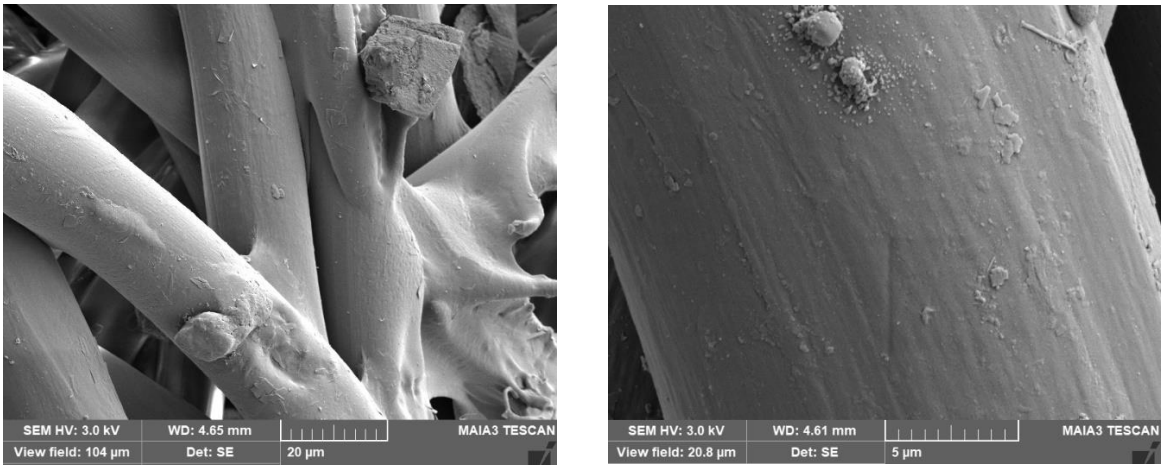

Sample 3

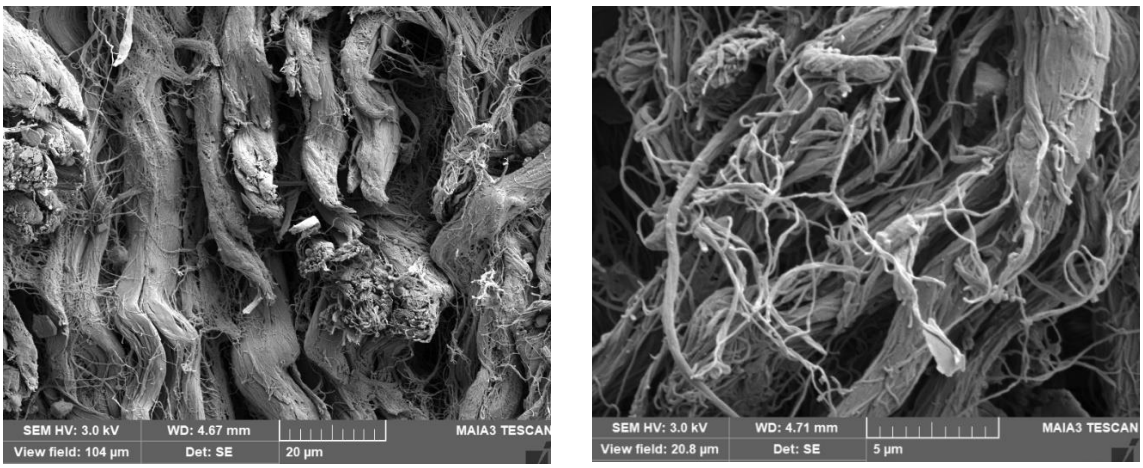

Sample 5

Figure 3. Micrographs of selected original samples taken at lower (left) and higher (right) magnification.

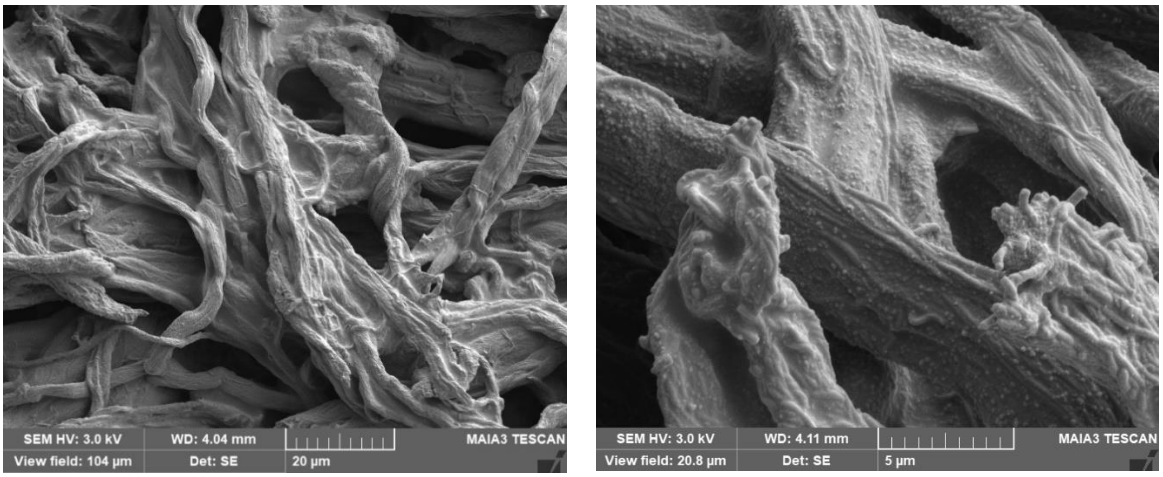

Sample 1

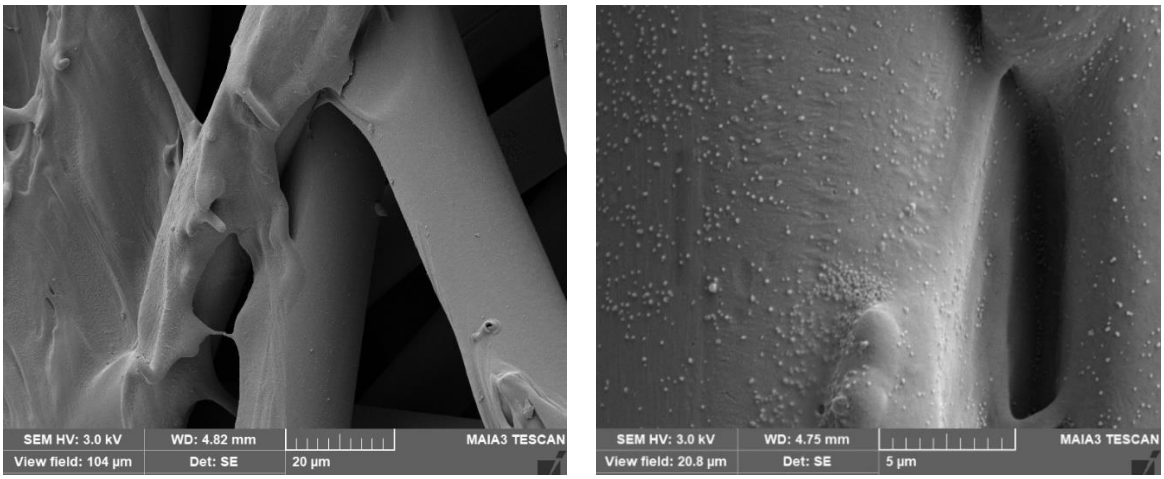

Sample 3

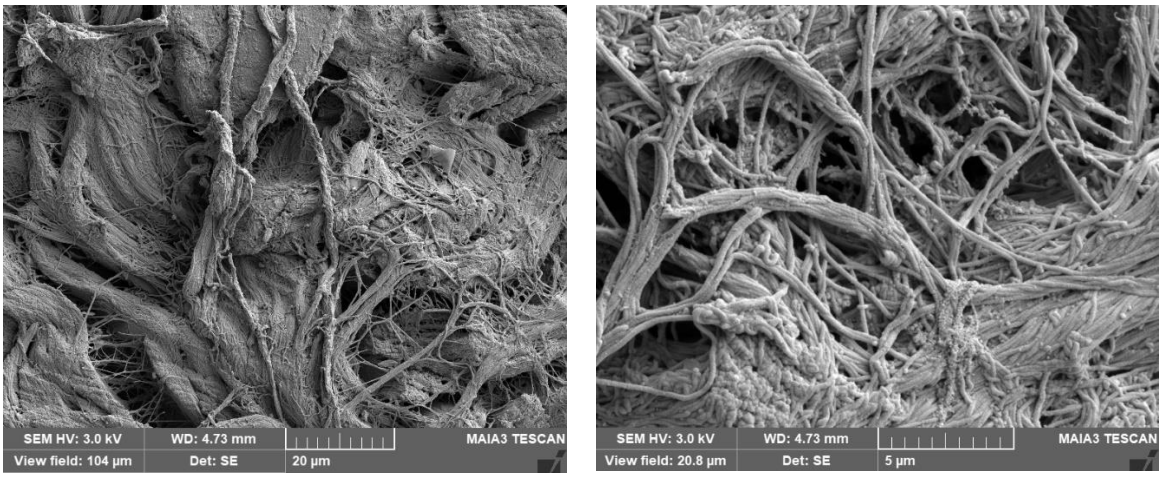

Sample 5

Figure 4 Micrographs the selected samples after coating with polyaniline taken at lower (left) and higher (right) magnification.

3.2. Coating thickness

The thickness of conducting layers in leather is an important parameter to assist in understanding of electrical properties of polyaniline-coated samples (Table 1). Calculations of the thickness was based on the analysis of optical images of sample cross-section (Figure 5). The thickness of the coated layers for all samples significantly varied for the smoother top and rougher bottom sides. Polyaniline layer was always thicker at the top than that on the reverse side. As mentioned above, the thickness is generally predetermined by the material hydrophilicity and consequent penetrability of the aqueous reaction mixture into the interior of leather. In the present case, the thickness is determined by depth to which reaction mixture was able to diffuse in about 20 min time needed for the polymerization of aniline. The conducting layer thickness could be increased either by the reduction of the reactant concentrations and consequent slowdown of the polymerization rate, or by the pre-swelling of leather with water.

Table 1. Thickness of polyaniline-penetrated layer, d, sample resistivity, ρ, sheet resistance, R_s, and transverse resistance,[a] R_t. T = smoother top side, B = rougher bottom side. ΔR is average relative resistance change in the bending test (500 cycles). Antibacterial activity against *Staphylococcus aureus*, A_{SA}, and *Klebsiella pneumoniae*, A_{KP}: ++ = good, + = moderate, 0 = none.

Leather		***d*, µm**	**ρ, kΩ cm**	**R_s, kΩ sq^{-1}**	**R_t, kΩ[a]**	**ΔR. %**	**A_{SA}**	**A_{KP}**
1– purple goatskin	T	86±4	0.877[b]	12±3	16500–18000	6–7	0	0
	B	45±6		21600±3500				
2–yellow-green pigskin	T	212±34	23.6[b]	204±23	>100 000	2–4	+	++
	B	132±17		252±10				
3–gambrela diabetic mat	T	903±42	0.478[b]	6.5±1.0	363–397	8–10	+	+
	B			4.9±1.0				
4–light beige pigskin	T	65±7	5.12	224±43	14300–15500	5–7	0	0
	B	59±10	9.71	130±4				
5–natural beige pigskin	T	166±4	2.77	92±34	519–549	1–2	0	+
	B	24±4	2.47	33±0.2				

[a] Sample size 0.5×1 cm^2. [b] About the same on both sides.

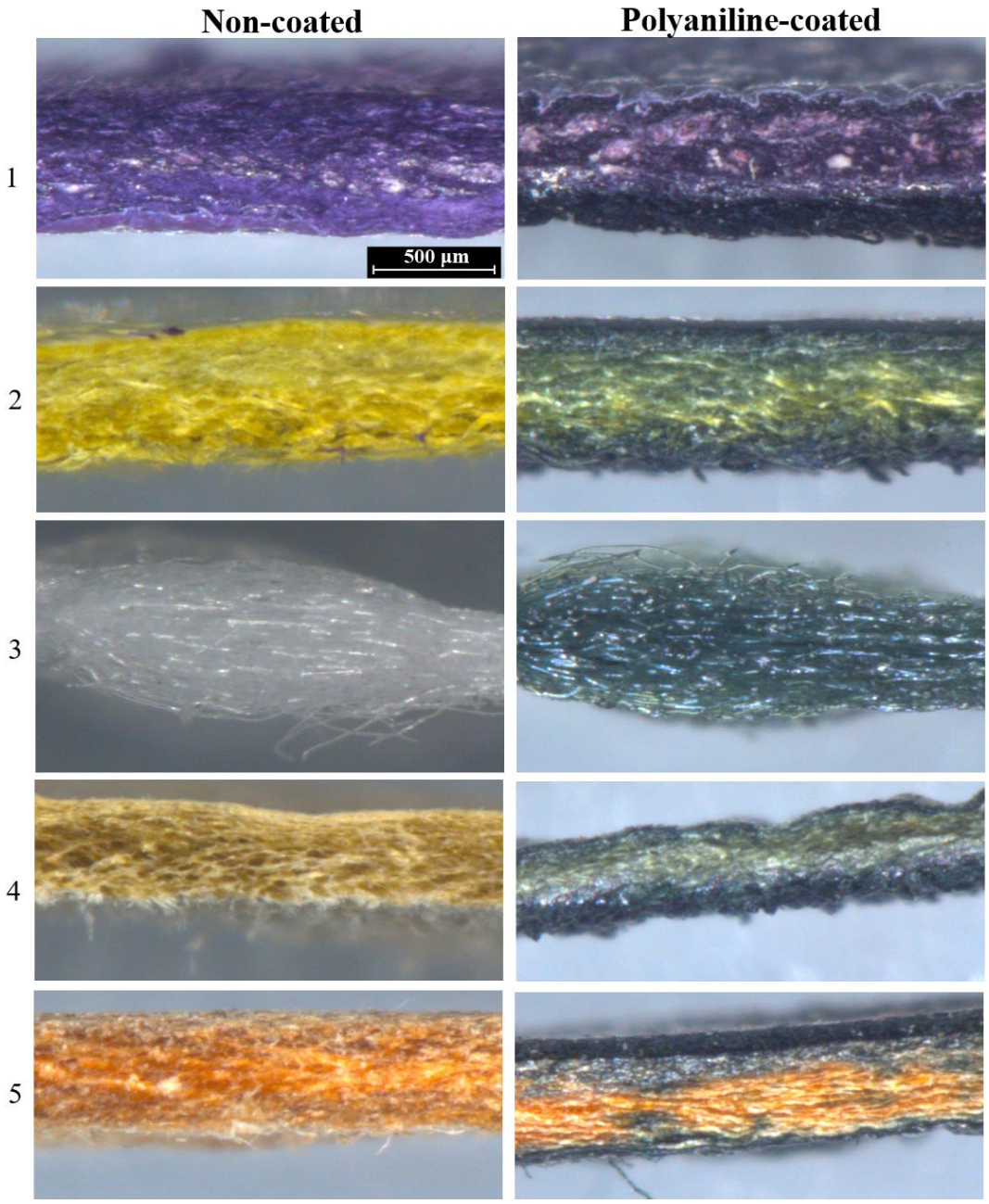

Figure 5. Cross-sectional optical images of original substrates (left, non-coated) and polyaniline-coated ones (right).

3.3. FTIR spectra

ATR FTIR spectroscopy is a non-destructive and non-invasive method consolidated for the analysis of the molecular structure of collagen-based materials. Collagen is one of the major components of skin. The collagen structure consists of three polypeptide chains organized in a triple helical conformation [19]. ATR FTIR spectra of non-coated leathers (Figure 6a) for samples 1 (based on goatskin), 2, 4 and 5 (based on pigskin) recorded from bottom side display a broad band from 3700 to 3000 cm^{-1} of hydroxyl group stretching vibrations overlapped with

Amide A band with maximum at 3322 cm^{-1} of N–H stretching vibrations, which are involved in hydrogen bonding in collagen triplet helical structure. In the spectrum of sample 3 (based on gambrela diabetic insole mat) the broad band of hydroxyl is missing and the Amide A band is shifted to 3297 cm^{-1}. The maxima observed at 3080 (overtone of Amide II band), 2965 (missing in the spectrum of sample 1), 2926, and 2856 cm^{-1} are attributed to the C–H stretching vibrations. Two major bands, the Amide I (mainly associated with the C=O stretching vibrations) and the Amide II (results from N–H bending vibrations and from C–N stretching vibrations) are situated at 1651 and 1553 cm^{-1} in the spectra of samples 1 (bottom), 2 (top and bottom), 4 (bottom), and 5 (top and bottom). In the spectrum of sample 3 they are shifted to the lower wavenumbers. The Amide III band (a very complex band depending on the nature of side chains and hydrogen bonding) is situated at about 1252 cm^{-1}. The spectrum of sample 3 (top and bottom) is close to the spectrum of polyamide from the spectral library.

The ATR FTIR spectra of samples 1 and 4 taken from the top side differ from the spectra of other samples. They exhibit some additional (sample 1) or just new bands (sample 4). The spectra are close to the spectrum of polyacrylate with maxima at 1735 cm^{-1} (C=O stretching vibrations), 1452 and 1378 cm^{-1} (C–H deformation vibration), 1280 and 1164 cm^{-1} (C–O stretching vibrations), and 1109 cm^{-1}. This signifies that the top side of these samples is coated with a synthetic polyacrylate overlayer.

After deposition of polyaniline the bands of polymer overlap the bands of leathers which are still well observed in the ATR FTIR spectra (Figure 6b) since the depth of penetration of the ATR FTIR spectroscopic method is several micrometres while the thickness of the polyaniline film deposited on collagen fibers obtained by in-situ dispersion mode is hundreds of nanometres. The bands of polyaniline observed at 1546 and 1459 cm^{-1} (quinonoid and benzenoid ring-stretching vibrations) are very close to the bands at 1553 and 1452 cm^{-1} of Amid I and Amid II of collagen in leather (Figure 6a). The bands situated at 1290 and 1242 cm^{-1} (characteristic for π-electron delocalization induced in the spectrum of polyaniline by protonation and of $C{\sim}N^{+\bullet}$ stretching vibrations in the polaronic structure) are well distinguished in the spectra of samples 1 (bottom), 4 (bottom), 5 (top), and 5 (bottom). Enhancement of absorption is observed about the maximum at 1098 cm^{-1} assigned to the vibrations of the $–NH^{+}=$ structure of protonated polyaniline. The peak at 797 cm^{-1} (C–H aromatic ring out-of-plane deformation vibrations in the *para*-disubstituted ring) is well detected in the spectra of coated leathers. Increased absorption in the region above 2000 cm^{-1} support the presence of polaron band in conducting form of polyaniline [2].

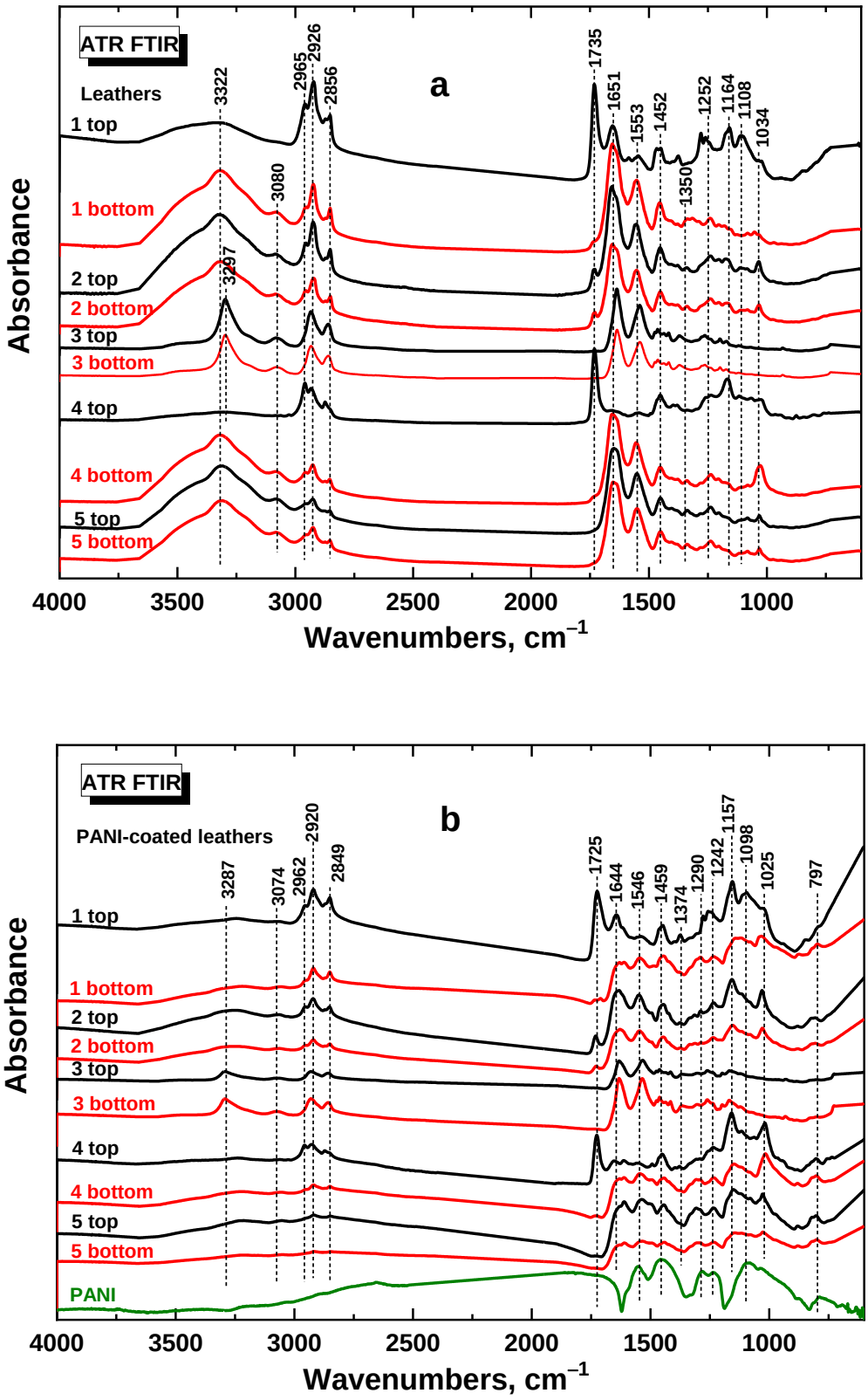

Figure 6. ATR FTIR spectra of leathers (a) before and (b) after coating with polyaniline recorded on top (in black) and bottom sides (in red). The spectrum of polyaniline (PANI, in green) is included for comparison.

3.4. Raman spectra

The Raman spectra of original leathers exhibit intensive fluorescence when 780 nm excitation wavelength has been used. The energy of this excitation is in resonance with the energy of electronic transition in polyaniline and only the contribution of polyaniline surface to Raman spectra is visible (Figure 7) [20]. The absence of the collagen features in the spectra also confirms good coating of individual fibers with polyaniline. The bands of polyaniline at 1585 cm^{-1} (C=C stretching vibrations in a quinonoid ring), at 1503 cm^{-1} (N–H deformation vibrations associated with the semiquinonoid structures), at 1337 cm^{-1} ($C{\sim}N^{+\bullet}$ vibrations of delocalized polaronic structures), at 1258 cm^{-1} (benzene-ring deformation vibrations), at 1171 cm^{-1} (C–H in-plane bending vibrations of the semi-quinonoid or benzenoid rings), and at 810 cm^{-1} (benzene-ring deformations) are well detected in the all spectra of polyaniline-coated leathers. Other peaks at 715, 640, 587, 517 and 418 cm^{-1} are linked with various amine in-plane deformation vibrations of the emeraldine salt structure or out-of-plane deformations of the ring [2].

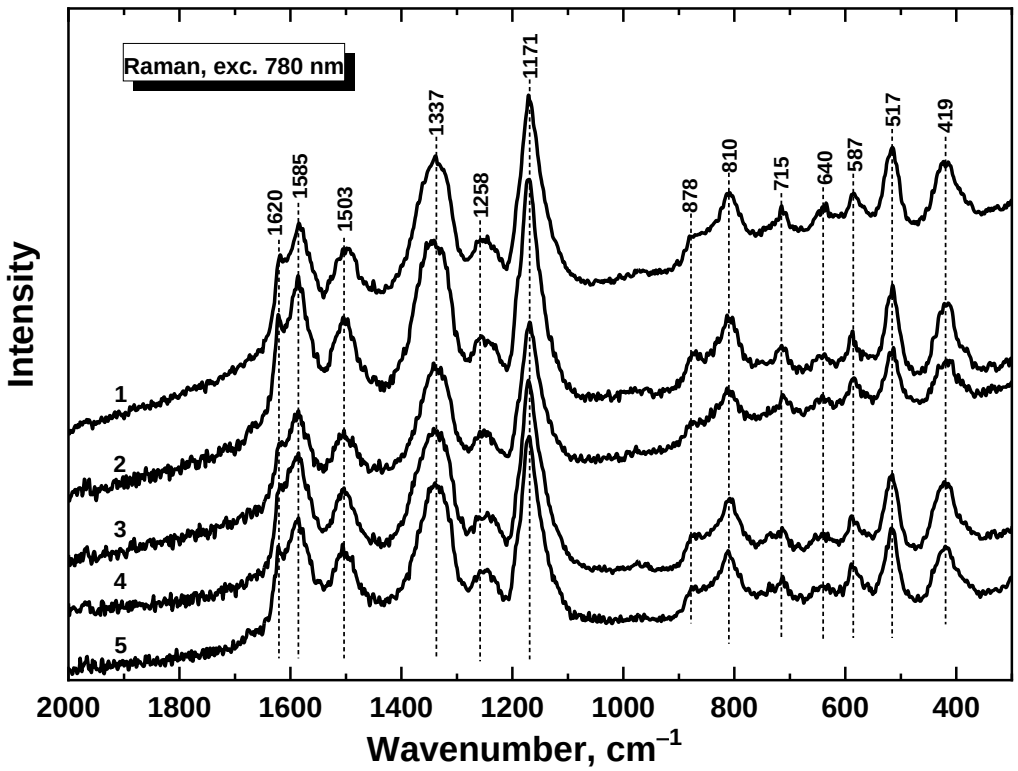

Figure 7. Raman spectra of polyaniline-coated leathers.

3.5. Resistivity

Polyaniline-coated leathers are materials with complex organic microstructure, which is not homogeneous. For that reason, electrical characterization cannot provide a single universal value of resistivity of any type, in the contrast to homogeneous inorganic materials. The results reported below (Table 1) thus have to be regarded as trends guiding the specific applications rather than rigorous physical parameters.

The resistivity ρ was determined by the four-point van der Pauw method. All samples were conducting, their resistivity being in the range 0.478–23.6×10^3 Ω cm. The application of this method, however, assumes the macroscopic homogeneity of the characterized materials, a condition which is obviously not satisfied by present samples (Figure 5). For the reason, they values of resistivity have only an indicative character.

The transverse resistance R_t was determined by a two-point method (Table 1). Low values (samples 3 and 5) indicate that the conducting polyaniline phase at least locally penetrates the leather profile and short-cuts the top and bottom surfaces. On the contrary, the high resistance (sample 2) means that both polyaniline layers are separated by insulating uncoated region.

3.6. Sheet resistance

Since the material has a layered inhomogeneous structure made of two materials with vastly different conductivity, the conducting phase being deposited only as a thin surface layer, electrical properties of the specimens have been further characterized by their sheet resistances R_s (Table 1) for both sides of the sheets. The top side points to the markedly smoother and shinier surface. The values represent the averages obtained by four-probe measurements at three different locations of the inner area of the sample surface. The relatively large experimental error (Table 1) stems from the differences in the sheet resistance measured at different places of the surface. Surprisingly, the top not always yielded more conducting surface; particularly samples 4 and 5 have lower sheet resistance on their dull side. The sample 3 was the most conducting on both sides, showing also the best homogeneity of the surface resistance over the surface.

3.7. Resistance during bending cycles

Considering the potential application in footwear products, the samples have been tested for the electrical wear by mechanical bending over 500 cycles under the angle of 10° with a

cycle duration 20 s. An example of 3.5 cycles (7 half-cycles) was extracted to illustrate the method (Figure 8a). Several interesting phenomena could be observed from this detailed measurement.

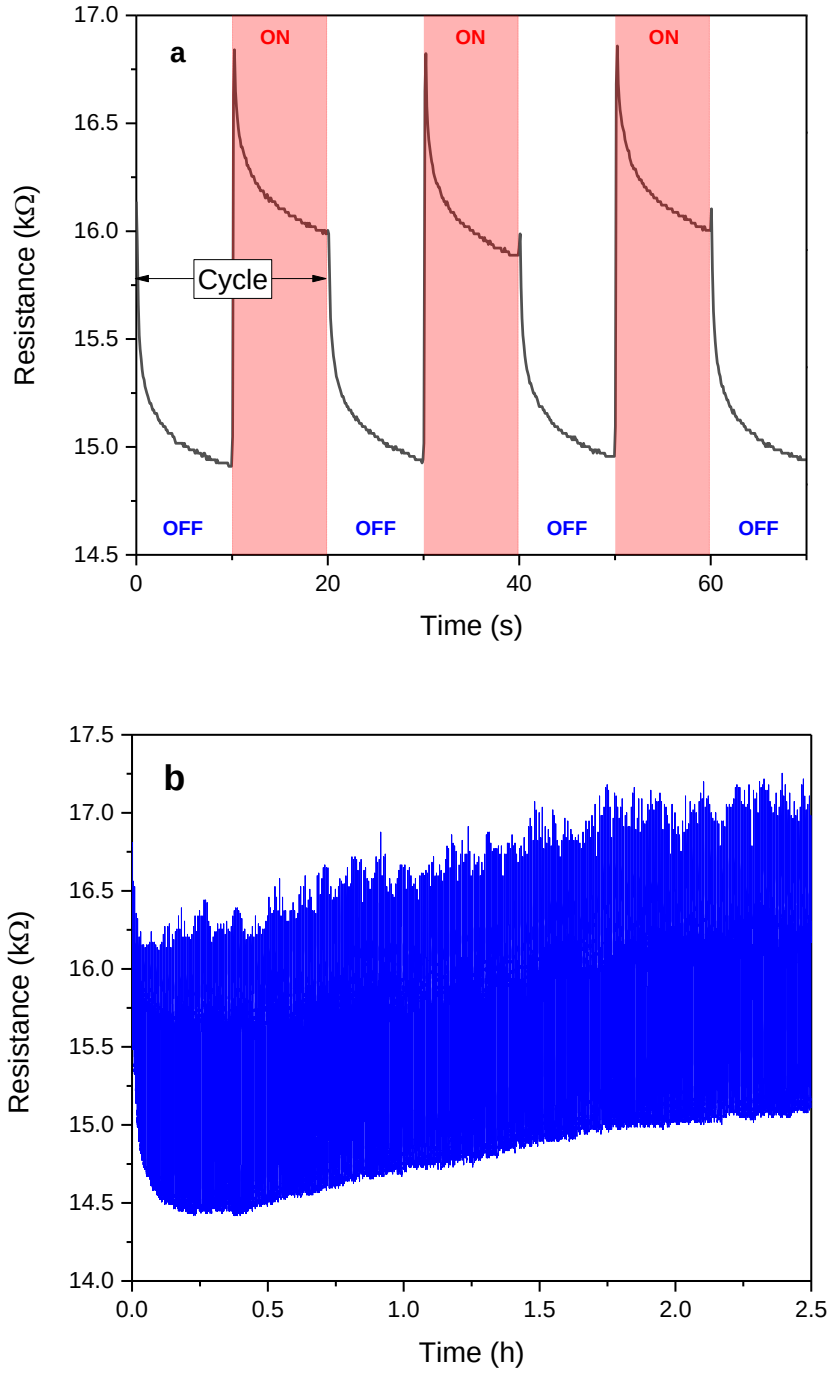

Figure 8. (a) The bending cycle of sample 1. OFF column is the time interval where the sample was not mechanically bended, ON column is the time interval where the sample was bended to 10°. (b) The bending of sample 1 over 500 cycles, each 20 s duration, 10° angle.

The response on the step-change of the mechanical stress caused by sudden change of the servo-motor position is very swift (~250 ms) reaching its maxima of resistance at the beginning and then slowly relaxes and stabilizes. After the pre-set time (here 10 s), the stress is released, and the leather layer quickly recovers its original resistance. The relaxation of the sample under the stress indicates that the mechanical stress does not affect leather equally. From the microscopic point of view, it is localized creating point narrowing of the fibres which later slowly spread out the stress thorough the material. This behaviour is probably the consequence of collagen inhomogeneity and differences in the size and thickness of fibres. When the mechanical stress is released, a small peak at the beginning of this half-cycle may arise. Its origin is not completely clear, but it may indicate a small increase in the distance of fibres (the loss of electrical contacts) due to the material pressing caused by fast return of the servo-motor to its original position.

The long-term cyclic bending of the leather samples over 500 cycles gives another interesting insight into the structure of the material (Figure 8b). Processing of these data and extracting resistances of the leather sample in non-bended and bended states revealed a slow drift of both quantities toward higher values which may indicate a slow wear of conductive layer (Figure 9). However, relative change of resistance calculated for n-th cycle as ΔR_n (%) = $[(R_{ON(n)} - R_{OFF(n)})/R_{OFF(n)}]\times 100$ indicates stable change between 5–8 % after half an hour for sample 1 and 8–10% for sample 3, which means that the leather sample is softened during the first half an hour and then it remains relatively stable. The comparison of relative resistance changes (Table 1) reveals that, according to the expectation, that pigskins (samples 2,4,5) contrary to the goatskin (sample 1) are generally stiffer resulting in lower resistance changes after bending. Soft goatskin behaves similarly to the gambrela (sample 3).

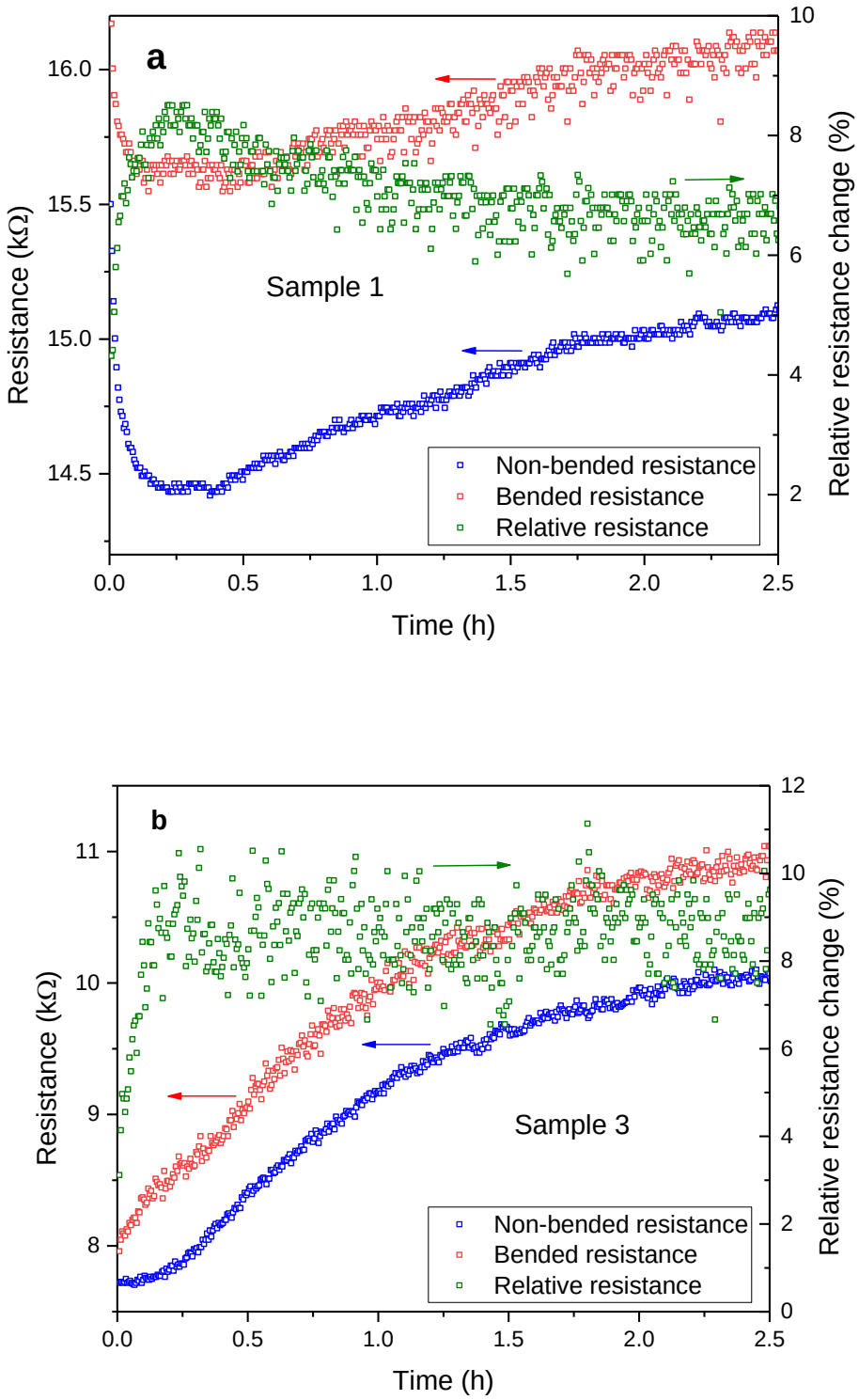

Figure 9. The 500 bending cycles (duration 10 s, angle of bending 10°) of (a) sample 1 and (b) sample 3. Blue and red squares represent non-bended and bended stated, respectively. Green symbols are calculated relative changes of resistance for each bending cycle.

3.8. Antibacterial activity

The polyaniline-coated leathers are considered for the application in the footwear industry. In addition to electrical properties, also antibacterial properties have therefore been tested. Polyaniline has often been reported to have various degrees on antibacterial action for various bacterial strains [21–23]. Conducting polymers are known to be efficient photocatalysts used for the removal of pollutant organic dyes from wastewaters [24]. The dye decomposition is explained by their interaction with photogenerated active peroxide species in water that are responsible also for the antibacterial performance.

The antibacterial effect of non-coated and polyaniline-coated leathers was studied using the agar plate disc diffusion method (Table 1). In accordance with ČSN 79 3880 Czech standard, in the case of a leather sample for which the bacterial growth percent is less than 25%, the antibacterial effect of the sample is regarded as positive. Whereas, ranges between 25 and 40% indicate that the antibacterial effect is considered moderate and more than 40% depicts no antibacterial effect [25]. The growth percent results for the evaluated samples revealed that the polyaniline-coated leathers, particularly samples 2 and 3, presented moderate activity against the two bacterial strains (*S. aureus* and *K. pneumoniae*) as compared to non-coated samples that show no antibacterial effect (Figure 10). Therefore, the coated leather samples displayed moderate level of antibacterial activity and the obtained results suggests that with improved modification the coated samples will show improved antibacterial properties.

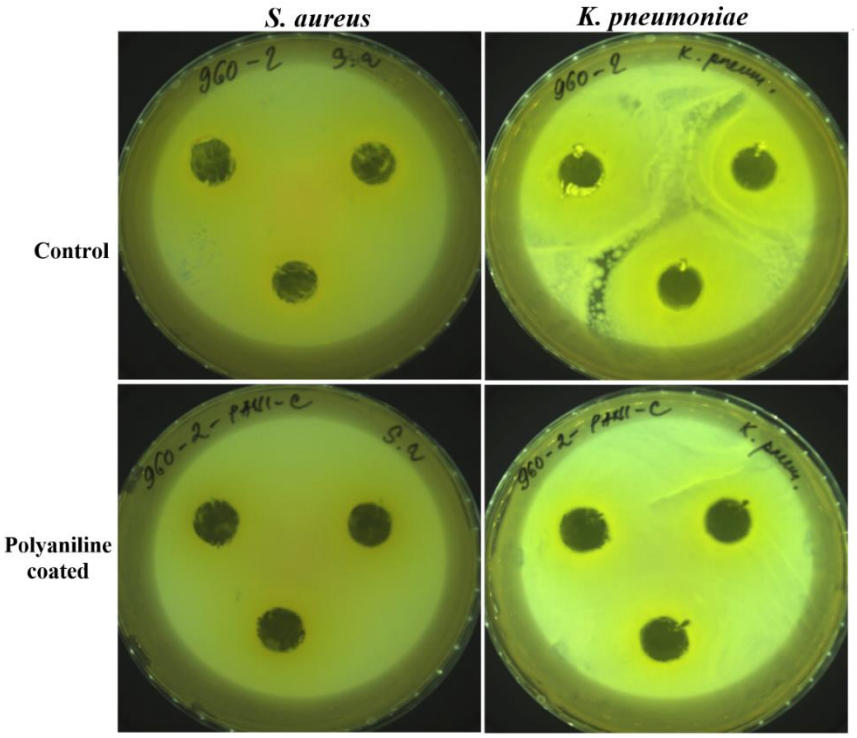

Figure 10. Images of inoculated agar plates after 24 h for the original leather 2 (as the control) and polyaniline-coated leather 2 demonstrating the growth density of *Staphylococcus aureus* and *Klebsiella pneumoniae* bacterial strains.

4. Conclusions

Various leathers were coated with a conducting polyaniline. As expected from natural materials, the fibrous microstructure differed depending on the source of leather and its processing, the face and rear sides being also different due to the leather finishing. As a consequence, the electrical properties varied, the typical sheet resistance being of the order of units to hundreds kΩ $\square^{-1}$, the difference between top and bottom sides was usually within the same order of magnitude. The traverse resistance of the order of 10^2 kΩ cm in some samples indicated the short-cut between top and bottom surfaces afforded by penetrating polyaniline phase. The changes in resistance during bending tests have been monitored with a lab-made apparatus designed for this study. The decrease in the units of percent has been observed after mechanical cycling. Original leathers displayed no antibacterial properties but some of them achieved this property after coating with polyaniline. The conducting leathers thus may be considered for the application in the shoe/footwear industry as antistatic materials or objects that could be heated by passing current. The decorative role of polyaniline coating could also be of interest.

Declaration of competing interest

The authors declare no competing interest.

Authors contribution statement

Fahanwi Asabuwa Ngwabebhoh: Data curation, formal analysis, writing - original draft. **Oyunchimeg Zandraa:** Data curation, formal analysis. **Tomáš Sáha:** Methodology, data curation. **Jaroslav Stejskal:** Conceptualization, methodology, data curation, supervision, writing - original draft. **Jiří Pfleger:** Data analysis, investigation. **Miroslava Trchová:** Methodology, investigation, writing - review & editing. **Dušan Kopecký:** Data curation, writing - review & editing. **Jan Prokeš:** Formal analysis. investigation.

Acknowledgments

The support of the project funded by the Tomas Bata University in Zlin (TP01010006) and co-financed with the support of the Technology Agency of the Czech Republic within the GAMA 2 programme.

ORCID

Fahanwi Asabuwa Ngwabebhoh – orcid.org/0000-0002-1492-1869
Oyunchimeg Zandraa – orcid.org/0000-0002-5330-6906
Tomáš Sáha - orcid.org/0000-0002-8091-8481
Jaroslav Stejskal – orcid.org/0000-0001-9350-9647
Jiří Pfleger – orcid.org/0000-0001-9576-7551
Miroslava Trchová – orcid.org/0000-0001-6105-7578
Dušan Kopecký – orcid.org/0000-0003-2813-7343
Jan Prokeš – orcid.org/0000-0002-8635-7056

References

[1] R. Gangopadhyay, A. De. Conducting polymer nanocomposites: A brief overview. Chem. Mater. 12 (2000) 608–622. doi: 10.1021/cm990537f

[2] J. Stejskal, M. Trchová, P. Bober, P. Humpolíček, V. Kašpárková, I. Sapurina, M.A. Shishov, M. Varga M. Conducting Polymers: Polyaniline. In: Encyclopedia of Polymer Science and Technology, Wiley online library, 2015. doi: 10.1002/0471440264.pst640.

[3] G.A. Snook, P. Kao, A.S. Best. Conducting-polymer-based supercapacitor devices and electrodes. J. Power Sources 196 (2011) 1–12. doi: 10.1016/j.jpowsour.2010.06.084

[4] J. Stejskal. Conducting polymers are not just conducting: a perspective for emerging technology. Polym. Int. 69 (2020):662–664. doi: 10.1002/pi.5947

[5] T.R. Zhang, S.L. Zeng, H. Jiang, Z.S. Li, D.Y. Bai, Y.J. Li, J.J. Li. Leather solid waste/poly(vinyl alcohol)/polyaniline aerogel with mechanical robustness, flame retardancy, and enhanced electromagnetic interference shielding. ACS Appl. Mater. Interfaces 13 (2021) 11332–11343. 10.1021/acsami.1c00880.

[6] V. Grm, D. Zavec, G. Dražić. A carbon-nanotubes-based heating fabric composite for automotive applications. Materiali Tehnologije 54 (2020) 761–768. doi: 10.17222/mit.2019.238

[7] K. Zhang, N.W. Kang, B. Zhang, R.J. Xie, J.Y. Zhu, B.H. Zou, Y.H. Liu, Y.Y. Chen, W. Shi, W.N. Zhang, W. Huang, J.S. Wu, F.W. Huo. Skin conformal and antibacterial PPy-leather electrode for ECG monitoring. Adv Electron Mater 6 (2020) 2000259. doi: 10.1002/aelm.202000259.

[8] J.D. Wegene, P. Thanikaivelan. Conducting leathers for smart product applications. Ind. Eng. Chem. Res. 53 (2014) 18209–18215. doi: 10.1021/ie503956p

[9] W.J. Demisie, T. Palanisamy, K. Kaliappa, P. Kavati, C. Bangaru. Concurrent genesis of color and electrical conductivity in leathers through in-situ polymerization of aniline for smart product applications. Polym. Adv. Technol. 26 (2015) 521–527. doi: 10.1002/pat.3483

[10] J. Stejskal, I. Sapurina. Polyaniline: Thin films and colloidal dispersions (IUPAC technical report). Pure Appl. Chem. 77 (2005) 815–826. doi: 10.1351/pac200577050815

[11] F.A. Ngwabebhoh, N. Saha, H.T. Nguyen, U.V. Brodnjak, T. Sáha, A. Lengalová, P. Sáha. Preparation and characterization of nonwoven fibrous biocomposites for footwear components. Polymers 12 (2020) 3016. doi: 10.3390/polym12123016

[12] N. Maráková, P. Humpolíček, V. Kašpárková, Z. Capáková, L. Martinková, P. Bober, M. Trchová, J. Stejskal. Antimicrobial activity and cytotoxicity of cotton fabric coated with conducting polymers, polyaniline or polypyrrole, and with deposited silver nanoparticles. Appl. Surf. Sci. 396 (2017) 169–176. doi:10.1016/j.apsusc.2016.11.024

[13] J. Yu, Z. Pang, J. Zhang, H. Zhou, Q. Wei. Conductivity and antibacterial properties of wool fabrics finished by polyaniline/chitosan. Colloid Surf. A, Physicochem. Eng. Asp. 548 (2018) 117–124. doi:10.1016/j.colsurfa.2018.03.065

[14] A. Riede, M. Helmstedt, I. Sapurina, J. Stejskal. In situ polymerized polyaniline films 4. Film formation in dispersion polymerization of aniline. J. Colloid Interface Sci 248 (2002) 413–418. doi: 10.1006/jcis.2001.8197

[15] J. Stejskal, I. Sapurina. On the origin of colloidal particles in the dispersion polymerization of aniline. J. Colloid Interface Sci. 274 (2004) 489–495. doi: 10.1016/j.jcis.2004.02.053

[16] J. Stejskal, M. Trchová, H. Kasparyan, D. Kopecký, Z. Kolská, J. Prokeš, I. Křivka, J. Vajďák, P. Humpolíček. Pressure-sensitive conducting and antibacterial materials obtained by *in-situ* dispersion coating of macroporous melamine sponges with polypyrrole. ACS Omega 6 (2021) 20895–20901. doi: 10.1021/acsomega.1c02330

[17] Y.F. Ma, W. Cheung, D.G. Wei, A. Bogozi, P.L. Chiu, L. Wang, F. Pontoriero, R. Mendelsohn, H.X. He. Improved conductivity of carbon nanotube networks by in situ

polymerization of a thin skin of conducting polymer. ACS Nano 2 (2008)1197–1204. doi: 10.1021/nn800201n

[18] J. Stejskal. Conducting polymer hydrogels. Chem. Pap. 71 (2017) 269–2291. doi: 10.1007/s11696-016-0072-9

[19] T. Riaz, R. Zeeshan, F. Zarif, K. IIyas, N. Muhammad, Z.F. Safi, A. Rahim, S.A.A. Rizvi, I.U. Rehman. FTIR analysis of natural and synthetic collagen. Appl. Spectrosc. Rev.. 53 (2018) 703–746. doi: 10.1080/05704928.2018.1426595

[20] M. Trchová, J. Stejskal. Resonance Raman spectroscopy of conducting polypyrrole nanotubes: disordered surface *versus* ordered body. J. Phys. Chem. A 122 (2018) 9298−9306. doi: 10.1021/acs.jpca.8b09794

[21] B.J. Li, W.J. Tang, D. Sun, B.B. Li, Y.X. Ge, X. Ye, W. Fang. Electrochemical manufacture of graphene oxide/polyaniline conductive membrane for antibacterial application and electrically enhanced water permeability. J. Membr. Sci. 640 (2021) 119844. doi: 10.1016/j.memsci.2021.119844

[22] Q. Pang, K.H. Wu, Z.L. Jiang, Z.W. Shi, Z.Z. Si, Q. Wang, Y.H. Cao, R.X. Hou, Y.B. Zhu. A polyaniline nanoparticles crosslinked hydrogel with excellent photothermal antibacterial and mechanical properties for wound dressing. Macromol. Biosci. 22 (2022) 2100386. doi: 10.1002/mabi.202100386

[23] F. Fenniche, A. Henni, Y. Khane, D. Aouf, N. Harfouche, S. Bensalem, D. Zerrouki, H. Belkhalfa. Electrochemical synthesis of reduced graphene oxide-wrapped polyaniline nanorods for improved photocatalytic and antibacterial activities. J. Inorg. Organometal. Polym. Mater. 32 (2022) 1011–1025. doi: 10.1007/s10904-021-02204-w

[24] J. Stejskal. Interaction of conducting polymers, polyaniline and polypyrrole, with organic dyes: polymer morphology control, dye adsorption and photocatalytic decomposition. Chem. Pap 74 (2020) 1–54. doi: 10.1007/s11696-019-00982-9].

[25] M.H. Salehi, H. Golbaten-Mofrad, S.H. Jafari, V. Goodarzi, M. Entezari, M. Hashemi, S. Zamanlui. Electrically conductive biocompatible composite aerogel based on nanofibrillated template of bacterial cellulose/polyaniline/nano-clay. Intl. J. Biol. Macromol. 173 (2021) 467–480. doi:10.1016/j.ijbiomac.2021.01.121

Graphical Abstract